Title	Electrochemical Behavior of Ti(III) Ions in Molten LiF–LiCl: Comparison with the Behavior in Molten KF–KCl
Author(s)	Norikawa, Yutaro; Yasuda, Kouji; Nohira, Toshiyuki
Citation	Journal of The Electrochemical Society (2020), 167(8)
Issue Date	2020-04-17
URL	http://hdl.handle.net/2433/250504
Right	
Type	Journal Article
Textversion	publisher

Journal of The Electrochemical Society

OPEN ACCESS

Electrochemical Behavior of Ti(III) Ions in Molten LiF–LiCl: Comparison with the Behavior in Molten KF–KCl

To cite this article: Yutaro Norikawa *et al* 2020 *J. Electrochem. Soc.* **167** 082502

Journal of The Electrochemical Society, 2020 **167** 082502

Electrochemical Behavior of Ti(III) Ions in Molten LiF–LiCl: Comparison with the Behavior in Molten KF–KCl

Yutaro Norikawa,[1] Kouji Yasuda,[2,3,*] and Toshiyuki Nohira[1,*,z]

[1]*Institute of Advanced Energy, Kyoto University, Gokasho, Uji, Kyoto 611-0011, Japan*
[2]*Agency for Health, Safety and Environment, Kyoto University, Sakyo-ku, Kyoto 606-8501, Japan*
[3]*Graduate School of Energy Science, Kyoto University, Sakyo-ku, Kyoto 606-8501, Japan*

Ti(III) ions has been prepared by the addition of 0.50 mol% of Li_2TiF_6 and 0.33 mol% of Ti sponge to LiF–LiCl melt, and their electrochemical behavior has been investigated using cyclic voltammetry and square wave voltammetry at 923 K. The reduction of Ti(III) ions to metallic Ti is observed around 1.2 V vs Li^+/Li, whereas the oxidation to Ti(IV) ions is observed at 2.78 V as a reversible electrochemical process. The diffusion coefficient of Ti(III) ions is determined to be 3.2×10^{-5} cm^2 s^{-1}. The electrochemical behavior of Ti(III) ions in LiF–LiCl melt is compared to that in KF–KCl melt. The potentials for Ti(IV)/Ti(III) and Ti(III)/Ti(0) couples based on the F_2/F^- potential in LiF–LiCl melt are more positive than those in KF–KCl melt by 0.41 V and 0.31 V, respectively. Such differences in potential are explained by the difference in interactions between Li^+–F^- and K^+–F^-.
 [DOI: 10.1149/1945-7111/ab8806]

Manuscript submitted February 12, 2020; revised manuscript received April 2, 2020. Published April 17, 2020.

Titanium metal has several excellent properties, such as a high specific strength, corrosion resistance, heat resistance, and biocompatibility. Despite these attractive properties, its high production cost and poor workability have prevented its widespread application. The electrodeposition of titanium has been proposed as a new manufacturing process to expand the applicability of titanium.

Plating titanium metal onto general substrates is one of the effective methods for utilizing the advantageous properties of titanium. Previous reports have shown that metallic titanium can be electrodeposited only from high-temperature molten salts as electrolytes.[1–31] Generally, chlorides,[1–13] fluorides,[14–18] and chloride–fluoride mixtures[19–31] have been used as the molten salt electrolytes for titanium electrodeposition. The morphology of the Ti deposits closely depends on the type of salts used as electrolyte. Compact and smooth films were generally difficult to obtain using chloride melts,[1–10] but could be obtained by using proper current densities or deposition potential in fluoride or chloride–fluoride melts.[5,14–27] Several researchers have discussed the effect of anions on the morphology of deposits and electrochemical behavior of Ti ions by changing the fluoride ion concentrations.[5,30–32] Takamura et al. reported that the morphology of deposits was improved by addition of LiF to LiCl–KCl melt at 773 K.[5] Song et al. reported that Ti metal with fine crystal grains was obtained when KF was added to NaCl–KCl at 1073 K.[31] Guangson et al. reported that Ti(II) ions were not observed and that Ti was deposited directly from Ti(III) ions when 10 wt% KF was added to KCl–NaCl–3 wt% K_2TiF_6.[32] Depositing Ti metal directly from Ti(III) ions is one of the characteristics of fluoride melts.[15–18] It has been previously suggested that the ionic state of Ti complex ions in the chloride–fluoride melts is similar to those in the all-fluoride melts. Although the effect of anions has been discussed in the above-mentioned papers, i.e. the effect of addition of fluoride ions to chloride melts on Ti electrodeposition, the effects of alkaline cations in chloride–fluoride melts have not been investigated. This is because molten salts containing multiple cations with a constant composition, like eutectic LiCl–KCl plus LiF, were used in these studies.

Based on this background, we focused on different fluoride–-chloride melt mixtures consisting of single cations to individually investigate the effect of alkaline cations. In this study, the electrochemical behavior of Ti(III) ions was investigated in LiF–LiCl melt (LiF:LiCl = 45:55 mol%) at 923 K. The effects of temperature and anion fraction were eliminated by using the same conditions as those used in our previous experiments conducted in KF–KCl eutectic melt (KF:KCl = 45:55 mol%) at 923 K,[25–27] which yielded electrodeposition of compact and smooth Ti. The redox potentials of Ti(III)/Ti(0) and Ti(IV)/Ti(III) were determined to be 0.33 and 1.82 V, respectively, vs K^+/K. In the present study, the redox potentials and diffusion coefficient of Ti(III) ions in LiF–LiCl were evaluated by using cyclic voltammetry and square wave voltammetry. The effect of cations in fluoride–chloride melt on the electrochemical behavior of Ti(III) ions was discussed by comparing the results obtained in LiF–LiCl and KF–KCl melts.

Experimental

Reagent-grade LiF (Kojundo Chemical Laboratory Co., Ltd., >99%) and LiCl (Kojundo Chemical Laboratory Co., Ltd., >99%) were dried under vacuum at 453 K for more than 72 h and at 773 K for 24 h. The salts were mixed in the prescribed composition (molar ratio of LiF:LiCl = 45:55, 300 g) and the mixture was loaded in a Ni crucible (Chiyoda Industry Manufacturing Plant Co., Ltd., outer diameter: 98 mm, inner diameter: 96 mm, height: 102 mm). The crucible was placed at the bottom of a stainless-steel vessel in an air-tight Kanthal container. The electrochemical measurements were conducted in dry Ar atmosphere at 923 K in a glove box. After blank measurements in molten LiF–LiCl, 0.50 mol% of Li_2TiF_6 and 0.33 mol% of Ti sponge (Kojundo Chemical Laboratory Co., Ltd., >99%) were added to the melt. Here, 0.33 mol% of Ti sponge corresponds to approximately twice the amount necessary to generate Ti(III) ions from 0.50 mol% of Li_2TiF_6, according to Eq. 1.

$$Ti(0) + 3Ti(IV) \rightarrow 4Ti(III) \quad [1]$$

Prior to the experiment, powdery Li_2TiF_6 was prepared from aqueous H_2TiF_6 solution (Morita Chemical Industry Co., Ltd., 40%) and Li_2CO_3 (FUJIFILM Wako Pure Chemical Co., Ltd., >99.0%), according to the method reported by Janz et al.[33] First, 37 g of Li_2CO_3 was added to 200 ml of aqueous H_2TiF_6 solution, and then ultrapure water was added to give a final volume of 300 ml.

$$H_2TiF_6 + Li_2CO_3 \rightarrow Li_2TiF_6 + CO_2 + H_2O \quad [2]$$

The Li_2TiF_6 product was completely soluble; therefore, any precipitate that formed was removed by filtration because it could contain impurities like TiO_2. Solid Li_2TiF_6 was recovered by evaporation of the solution under reduced pressure. The thus-

*Electrochemical Society Member.
zE-mail: nohira.toshiyuki.8r@kyoto-u.ac.jp

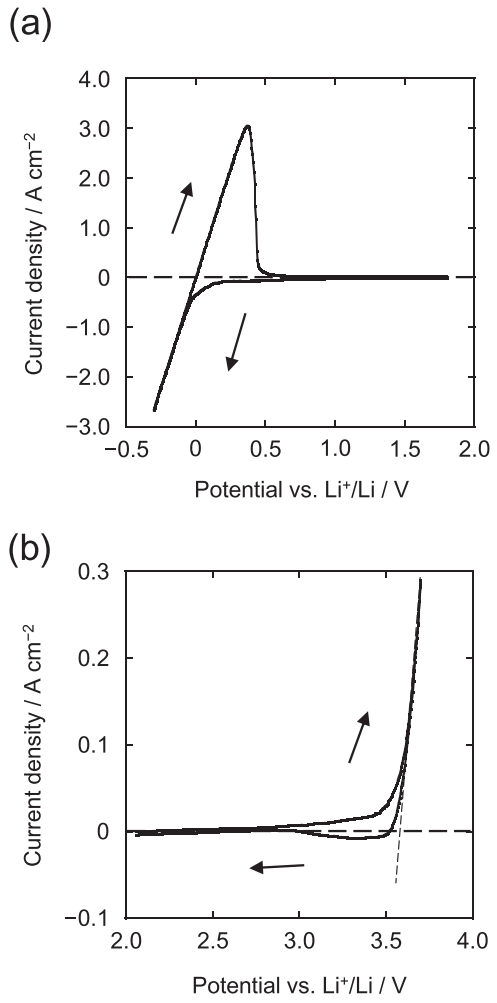

Figure 1. Cyclic voltammograms (a) in the negative potential region at a Mo flag electrode and (b) in the positive potential region at a glass-like carbon rod electrode in molten LiF–LiCl at 923 K. Scan rate: 0.5 V s^{-1}.

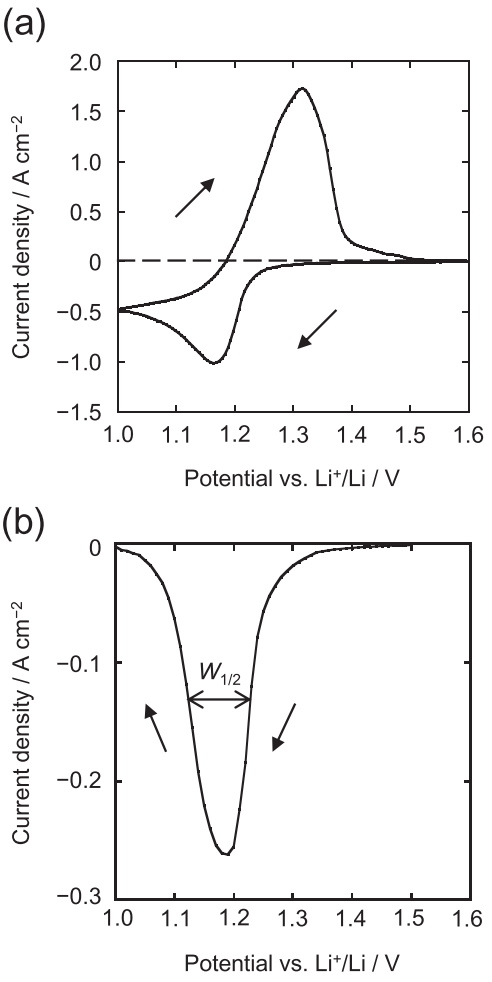

Figure 2. (a) Cyclic voltammogram and (b) square wave voltammogram at a Mo flag electrode in molten LiF–LiCl after the addition of Li_2TiF_6 (0.50 mol %) and Ti sponge (0.33 mol%) at 923 K. (a) Scan rate: 0.5 V s^{-1}. (b) f = 5 Hz, E_{SW} = 20 mV, and ΔE = 10 mV.

obtained Li_2TiF_6 was dried under vacuum at 453 K for over 6 h and pulverized in a mortar under dry Ar atmosphere in a glove box.

Electrochemical measurements and galvanostatic electrolysis were conducted by a three-electrode method using an electrochemical measurement system (Hokuto Denko Corp., HZ-7000). The working electrodes were Mo plate (Nilaco Corp., 10 mm × 10 mm, thickness: 0.1 mm, 99.95%), Mo flag (Nilaco Corp., diameter: 3.0 mm, thickness: 0.1 mm, 99.95%), Au flag (Nilaco Corp., diameter: 3.0 mm, thickness: 0.1 mm, 99.98%), and glassy carbon rod (Tokai Carbon Co., Ltd., diameter: 3.0 mm) electrodes. The structure of the flag electrodes was reported in our previous paper.[34] Ti rods (Nilaco Corp., diameter: 3.0 mm, 99.5%) were used as the counter and reference electrodes. In the blank measurement, a Pt wire (Nilaco Corp., diameter: 1.0 mm, 99.98%) was used as the quasi-reference electrode. The potential of the reference electrodes was calibrated with respect to a dynamic Li^+/Li potential, determined by cyclic voltammetry on a Mo electrode. When necessary, the potential was expressed based on Cl_2/Cl^- and F_2/F^- potentials, calculated from the theoretical decomposition voltage of the salt. The calibration method is explained in the next section. The melt temperature was measured using a type-K thermocouple. The salt adhering to the deposits was removed by ultrasonic washing in distilled water for 10 min.

The surface and cross-section of the sample were observed by using scanning electron microscopy (SEM; Thermo Fisher Scientific Inc., Phenom Pro Generation 5). Before the observation of the cross section, the samples were embedded in an acrylic resin and polished with emery papers and buffing compounds. The samples were then coated with Au using an ion sputtering apparatus (Hitachi, Ltd., E-101) to impart conductivity. The deposits were also characterized by energy-dispersive X-ray (EDX; AMETEK Co. Ltd., EDAX Genesis APEX2) and X-ray diffraction (XRD; Rigaku Corp., Ultima IV, Cu-$K\alpha$ line) analyses. A small portion of the molten salt was sampled by the suction method using a borosilicate glass tube (Pyrex®, outer diameter: 6 mm, inner diameter: 4 mm) and dissolved in aqueous HNO_3 solution (pH 1, obtained from Tama Chemical Corp., AA-100 grade, 68 wt%). The solution was analyzed by using inductive coupled plasma-atomic emission spectroscopy (ICP-AES; Hitachi, Ltd., SPECTRO BLUE) to determine the Ti ion concentration in the sampled molten salt.

Results and Discussion

Electrochemical window of LiF–LiCl molten salt.—Prior to the measurement of Ti(III) ions in LiF–LiCl, the electrochemical window of the used molten LiF–LiCl at 923 K was determined. Figure 1a shows the cyclic voltammogram at a Mo flag electrode in a negative potential region. The cathodic current due to the formation of Li metal fog increases gradually from 0.2 V vs Li^+/Li. Then, the current increases rapidly from 0 V, corresponding to the deposition of liquid Li metal.

$$Li^+ + e^- \rightarrow Li(l) \qquad [3]$$

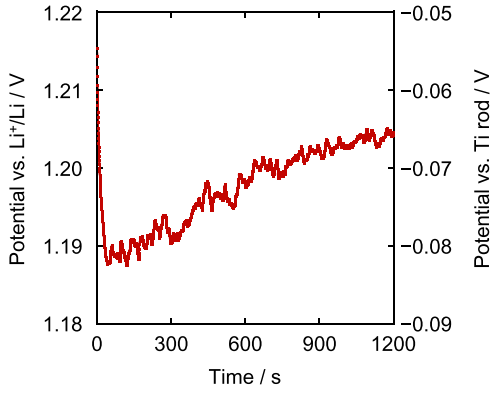

Figure 3. Potential transient curve obtained during galvanostatic electrolysis of a Mo plate electrode at -50 mA cm^{-2} for 20 min in LiF–LiCl after the addition of Li_2TiF_6 (0.50 mol%) and Ti sponge (0.33 mol%) at 923 K.

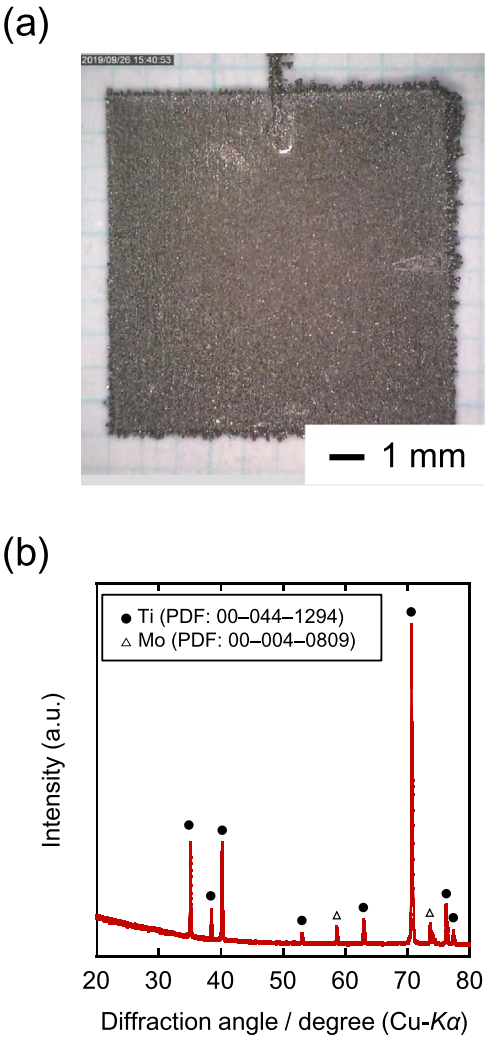

Figure 4. (a) Optical image and (b) XRD pattern of the sample obtained by galvanostatic electrolysis of a Mo plate electrode at -50 mA cm^{-2} for 20 min in molten LiF–LiCl after the addition of Li_2TiF_6 (0.50 mol%) and Ti sponge (0.33 mol%) at 923 K.

After reversal of the scan direction, anodic current due to Li metal dissolution was observed. The potential at zero current in the linear variation region during the positive sweep can be considered the redox potential of Li^+/Li. Figure 1b shows the cyclic voltammogram at a glass-like carbon electrode in a positive potential region. A sharp

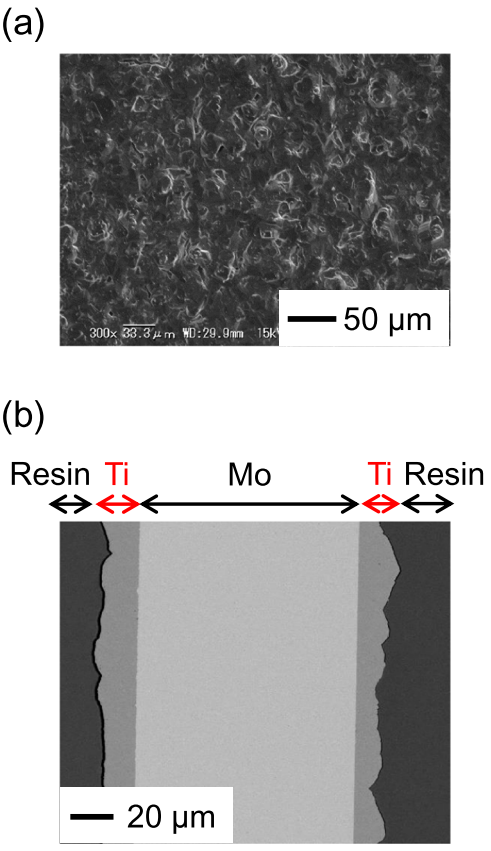

Figure 5. (a) Surface and (b) cross-sectional SEM images of the sample obtained by galvanostatic electrolysis of a Mo plate electrode at -50 mA cm^{-2} for 20 min in molten LiF–LiCl after the addition of Li_2TiF_6 (0.50 mol%) and Ti sponge (0.33 mol%) at 923 K.

increase in anodic current due to Cl_2 gas evolution is observed around 3.5 V.

$$2Cl^- \rightarrow Cl_2 + 2e^- \quad [4]$$

Based on this result, the electrochemical window of LiF–LiCl molten salt (LiF:LiCl = 45:55 mol%, 923 K) is determined to be 3.5 V. This value is in good agreement with the theoretical electrochemical window of LiF–LiCl, 3.51 V, which has been calculated from the standard Gibbs energy of formation of LiCl(*l*) (-333.81 kJ mol^{-1} at 923 K),[35] assuming the activity of LiCl to be 0.55.

Reduction of Ti(III) ions.—The electrochemical reduction of Ti (III) ions was investigated using cyclic voltammetry and square wave voltammetry. Figure 2a shows the cyclic voltammogram in a negative potential region at a Mo flag electrode in molten LiF–LiCl after the addition of 0.50 mol% of Li_2TiF_6 and 0.33 mol% of Ti sponge at 923 K. Cathodic current increases from approximately 1.30 V vs Li^+/Li and forms a peak at 1.18 V. After reversal of the scanning direction at 1.00 V, the corresponding anodic current peak is observed at 1.31 V. For a more detailed analysis of the cathodic reaction, square wave voltammetry was conducted on the same melt. The square wave voltammogram obtained at $f = 5$ Hz, $E_{SW} = 20$ mV, and $\Delta E = 10$ mV (Fig. 2b) shows a single peak at 1.19 V vs Li^+/Li. Here, f is the frequency, E_{SW} is the amplitude of the SW pulses, and ΔE is the potential increment of a staircase potential ramp. In a square wave voltammogram, the half-width of a peak, $W_{1/2}$, is given by Eq. 5[36–39]

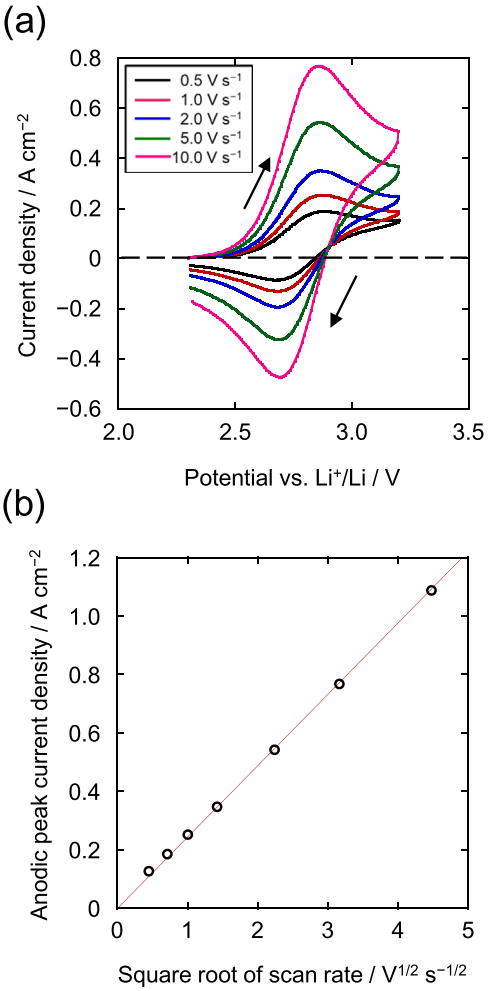

Figure 6. (a) Cyclic voltammograms at a Au flag electrode in molten LiF–LiCl after the addition of Li_2TiF_6 (0.50 mol%) and Ti sponge (0.33 mol %) at various scan rates at 923 K. (b) Dependence of anodic peak current density on scan rate.

$$W_{1/2} = \frac{RT}{nF}\left\{3.53 + 3.46\frac{\xi_{SW}^2}{\xi_{SW} + 8.1}\right\} \quad \xi_{SW} = \frac{nFE_{SW}}{RT} \qquad [5]$$

where R is the universal gas constant, T is the temperature, n is the number of electrons transferred, and F is the Faraday constant. The value n is calculated to be 3.0 from the peak half-width of 100 mV in Fig. 2b. Since the calculated value is 3.0, the reduction observed in the voltammogram in Fig. 2b is suggested to be due to deposition of Ti metal.

$$\mathrm{Ti(III)} + 3\mathrm{e}^- \rightarrow \mathrm{Ti(0)} \qquad [6]$$

To confirm this, galvanostatic electrolysis was conducted using the Mo plate electrode at a current density of $-50\ \mathrm{mA\ cm^{-2}}$ for 20 min. Figure 3 shows the potential transient curve during galvanostatic electrolysis. The potential during electrolysis was around 1.2 V vs Li^+/Li, indicating the progress of the cathodic reaction observed in the cyclic voltammogram. As shown in the right-hand potential axis, the potential was approximately −70 mV against a Ti reference electrode, which suggests the presence of concentration and activation overpotentials. The optical image of the sample after water washing (Fig. 4a) shows deposits having metallic luster covering the entire substrate. The XRD pattern of the sample (Fig. 4b) shows peaks only for metallic Ti and Ni substrate. Although LiF has low solubility in water (0.13 g per 100 g-H_2O at 293 K[40]), any adhered salts were successfully removed from the sample, likely because the dissolution of LiCl assisted the physical removal of LiF from the sample surface. Surface and cross-sectional SEM images of the sample are shown in Figs. 5a and 5b, respectively. The deposits have compact grains with diameters of approximately 10 μm. Only Ti was detected by EDX analysis of the sample surface. The cross-sectional SEM image demonstrates that adherent, compact, and comparably smooth films with a thickness of around 15 μm were electrodeposited on the Mo substrate. Based on these results, the cathodic wave in the cyclic voltammogram is assigned to the reduction of Ti(III) ions to metallic Ti (Eq. 6).

Oxidation of Ti(III) ions.—The anodic oxidation of Ti(III) ions was investigated using cyclic voltammetry. Figure 6a shows the cyclic voltammograms obtained at a Au flag electrode in a positive potential region. The scan rates were varied from $0.5\ \mathrm{V\ s^{-1}}$ to $10.0\ \mathrm{V\ s^{-1}}$. Pairs of redox currents are observed around 2.8 V vs Li^+/Li. This redox reaction is reversible because the peak potential was constant and independent of the scan rate. For a reversible reaction, the following relationship holds between the anodic peak potential (E_{ap}) and the cathodic peak potential (E_{cp}):[41]

$$E_{ap} - E_{cp} \cong 2.3RT/nF \qquad [7]$$

Since the difference of peak potentials in Fig. 6a is 0.16 V, n is calculated to be 1.1. Thus, the observed redox currents correspond to the redox reaction of Ti(IV)/Ti(III).

$$\mathrm{Ti(IV)} + \mathrm{e}^- \rightleftharpoons \mathrm{Ti(III)} \qquad [8]$$

Here, the formal potential, $E^{\circ\prime}$, is calculated to be 2.78 V from the average values of the cathodic and anodic peak potentials.

The diffusion coefficient of Ti(III) ions, $D_{Ti(III)}$, in LiF–LiCl molten salt was determined from the cyclic voltammetry results. In a reversible electrochemical reaction for the soluble reactants and products, the anodic peak current (I_{ap}) is given by Eq. 9,[41]

$$I_{ap} = 0.446FAc_{Ti(III)}(D_{Ti(III)}Fv/RT)^{1/2} \qquad [9]$$

where A is the electrode area and v is the scan rate. The volume concentration of ions in the electrolyte, $c_{Ti(III)}$, is calculated to be $2.88 \times 10^{-4}\ \mathrm{mol\ cm^{-3}}$ from the ICP-AES result for the LiF–LiCl melt and its density. In this case, the density of the melt with a composition of LiF:LiCl = 45:55 mol% is estimated to be $1.58\ \mathrm{g\ cm^{-3}}$ at 923 K by extrapolating the reported data for the

Table I. The formal potentials for Ti(IV)/Ti(III) couple determined by CV and the peak potentials in SWV for Ti(III)/Ti(0) couple in LiF–LiCl and KF–KCl.

	E vs Cl_2/Cl^-/V		E vs F_2/F^-/V			
Molten salt (Molar ratio)	Ti(IV)/Ti(III)	Ti(III)/Ti(0)	Ti(IV)/Ti(III)	Ti(III)/Ti(0)	T/K	References
LiF–LiCl (45:55)	−0.73[a)]	−2.32[b)]	−2.70[a)]	−4.29[b)]	923	This study
KF–KCl (45:55)	−1.81[a)]	−3.30[b)]	−3.11[a)]	−4.60[b)]	923	26

a) The formal potential determined by CV. b) The peak potential in SWV.

melts of compositions LiF:LiCl = 37:63 and 50:50 mol% in the temperature range 940–1260 K.[42] Figure 6b shows the plots of I_{ap} vs $v^{1/2}$ in the range 0.2–20.0 V s^{-1}. The value of $D_{Ti(III)}$ is determined from the slope of the plots to be 3.2×10^{-5} cm^2 s^{-1} at 923 K.

Comparison of electrochemical behavior of Ti(III) ions.— Table I compares the redox potentials for Ti(IV)/Ti(III) and Ti (III)/Ti(0) couples in LiF–LiCl and KF–KCl at 923 K. In the second and third columns of the table, the potentials are expressed against the Cl_2/Cl^- potential, in which the conversion of potential has been conducted using the theoretical electrochemical windows of the molten salts. The theoretical electrochemical window of LiF–LiCl is 3.51 V, as calculated in previous section, while that of KF–KCl is calculated to be 3.63 V based on the standard Gibbs energy of KCl(l) at 923 K.[35] The potentials for the Ti(IV)/Ti(III) and Ti(III)/Ti(0) couples in LiF–LiCl are more positive than those in KF–KCl by 1.08 V and 0.98 V based on Cl_2/Cl^- potential, respectively. In other words, the stable potential range of Ti(III) ions in LiF–LiCl shifts in the positive direction by ca. 1 V compared with the KF–KCl system.

To explain the shift in potential, we first must consider the stability of the titanium complex ions from the viewpoint of thermodynamics. Since hexacoordinated titanium ions exist in molten salts,[15,43–45] the possible titanium complex ions present in the fluoride–chloride molten salt mixture are $TiF_{6-x}Cl_x^{3-}$. To evaluate whether F^- or Cl^- anions coordinate more readily, the standard Gibbs energies for conversion from $TiCl_3$ to TiF_3 by the reaction with LiF or KF have been calculated based on the reported thermochemical data.[35]

$$TiCl_3(s) + 3LiF(l) = TiF_3(s) + 3LiCl(l) \quad [10]$$

$$\Delta G_C^o = -126.01 \text{ kJ mol}^{-1} \text{ at } 923 \text{ K}$$

$$TiCl_3(s) + 3KF(l) = TiF_3(s) + 3KCl(l) \quad [11]$$

$$\Delta G_C^o = -320.67 \text{ kJ mol}^{-1} \text{ at } 923 \text{ K}$$

Since the Gibbs energies of conversion have large negative values for both the systems, the most probable form of titanium complex ions is TiF_6^{3-}. When the ligands of the titanium complex ions are only F^-, its stability should be discussed based on the potential with reference to that of the F_2/F^- couple. Thus, the redox potentials for the Ti(IV)/Ti(III) and Ti(III)/Ti(0) couples in LiF–LiCl and KF–KCl against the F_2/F^- potential are also listed in Table I. The potential conversions have been conducted in the same manner as the conversion for the Cl_2/Cl^- potential. Although the difference in potential between LiF–LiCl and KF–KCl has decreased, there remain large differences of 0.41 V and 0.31 V for the Ti(IV)/Ti (III) and Ti(III)/Ti(0) couples, respectively.

Similar tendencies of the shifts in potential, i.e., more positive for smaller alkaline cation, were reported for pure chloride molten salts.[43,44] Table II compares the potentials for the Ti(IV)/Ti(III), Ti (III)/Ti(II), Ti(III)/Ti(0), and Ti(II)/Ti(0) couples in LiCl, LiCl–KCl, NaCl–CsCl, and CsCl molten salts at 1023 K, as reported by Song et al.[44] They explained that the potential shifts were due to the polarization power of alkaline cations, which was strongly related to cation radius. That is, smaller cations such as Li^+ have higher polarization power and strong ionic attraction to Cl^-, which results in less stable Ti chlorocomplexes. The present shifts in potential in fluoride–chloride molten salts are well explained in the same manner: the smaller cations that interact strongly with F^- reduce the stability of the Ti fluorocomplexes. For the preliminary quantitative discussion, the difference of Coulomb interactions between Ti^{3+}–F^- and A^+–F^- (A = Li and K) is roughly evaluated by following equation.[46]

$$\Delta\Phi = \Phi(Ti^{3+} - F^-) - \Phi(A^+ - F^-) = \frac{|Z_{Ti}Z_F|}{r_{Ti} + r_F} - \frac{|Z_A Z_F|}{r_A + r_F} \quad [12]$$

Here, r_{Ti}, r_A, and r_F are the 6-coordinated ionic radii for Ti^{3+}, A^+, and F^- proposed by Shannon, respectively,[47] and $Z_{Ti} = 3$, $Z_A = 1$, and $Z_F = -1$ are ionic valences. The calculated $\Delta\Phi$ are 1.13×10^{-2} pm^{-1} for the K system and 1.02×10^{-2} pm^{-1} for the Li system, which indicates the Coulomb force between Ti^{3+} and F^- in the K system is larger than that in the Li system. Furthermore, the difference in potential in fluoride–chloride melts is larger than that in pure chloride melts. For example, according to Tables I and II, the difference in potential for the Ti(IV)/Ti(III) couple was 0.41 V based on F_2/F^- potential between LiF–LiCl and KF–KCl, and 0.32 V based on Cl_2/Cl^- potential between LiCl and CsCl. The larger difference in fluoride–chloride melts is explained by the larger difference in interaction between Li^+–F^- and K^+–F^- than that between Li^+–Cl^- and Cs^+–Cl^-.

Conclusions

The electrochemical behavior of Ti(III) ions was investigated in LiF–LiCl melt after the addition of 0.50 mol% of Li_2TiF_6 and 0.33 mol% of Ti sponge at 923 K. The cathodic reaction at around 1.2 V vs Li^+/Li was determined to be the reduction of Ti(III) ions to Ti metal, based on the results of cyclic voltammetry, square wave voltammetry, and XRD analyses of the deposits. The oxidation reaction of Ti(III) ions to Ti(IV) ions was reversible, with the formal potential of 2.78 V. The diffusion coefficient of Ti(III) ions was determined to be 3.2×10^{-5} cm^2 s^{-1}. The potentials for Ti(III)/Ti(0) and Ti(VI)/Ti(III), with reference to the F_2/F^- potential in LiF–LiCl, were more positive than those in KF–KCl by 0.31 V and 0.41 V, respectively. Such potential differences were explained by the interactions of Li^+–F^- and K^+–F^-; smaller cations interacts more strongly with F^-, resulting in reduced stability of Ti fluorocomplexes.

Acknowledgments

A part of this study was conducted as a collaboration with Sumitomo Electric Industries, Ltd. A part of this work was supported by JSPS Fellows grant number 19J15015.

Table II. The formal potentials for Ti(IV)/Ti(III) couple determined by CV, and the peak potentials in SWV for Ti(III)/Ti(II), Ti(III)/Ti(0), and Ti (II)/Ti(0) couples in LiCl, LiCl–KCl, NaCl–CsCl and CsCl molten salts.[44]

	E vs Cl_2/Cl^-/V				
Molten salt (Molar ratio)	Ti(IV)/Ti(III)	Ti(III)/Ti(II)	Ti(II)/Ti(0)	Ti(III)/Ti(0)	T/K
LiCl	−0.30[a)]	−1.67[b)]	−1.98[b)]	—	1023
LiCl–KCl (59:41)	−0.43[a)]	−1.70[b)]	−2.01[b)]	—	1023
NaCl–CsCl (35:65)	−0.53[a)]	−1.88[b)]	−2.12[b)]	—	1023
CsCl	−0.62[a)]	—	—	−1.98[b)]	1023

a) The formal potential determined by CV. b) The peak potential in SWV.

ORCID

Kouji Yasuda https://orcid.org/0000-0001-5656-5359
Toshiyuki Nohira https://orcid.org/0000-0002-4053-554X

References

1. M. B. Alpert, F. J. Schultz, and W. F. Sullivan, *J. Electrochem. Soc.*, **104**, 555 (1957).
2. B. J. Fortin, J. G. Wurm, L. Gravel, and R. J. A. Potvin, *J. Electrochem. Soc.*, **106**, 428 (1959).
3. A. Menzies, D. L. Hill, G. J. Hills, L. Young, and J. O. M. Bockris, *J. Electroanal. Chem.*, **1**, 161 (1959).
4. G. M. Haarberg, W. Rolland, A. Sterten, and J. Thonstad, *J. Appl. Electrochem.*, **23**, 217 (1993).
5. H. Takamura, I. Ohno, and H. Numata, *J. Jpn. Inst. Metals*, **60**, 388 (1996).
6. X. Ning, H. Asheim, H. Ren, S. Jiao, and H. Zhu, *Metall. Mater. Trans. B*, **42**, 1181 (2011).
7. T. Yuan, Q.-G. Weng, Z. Zhou, J. Li, and Y.-H. He, *Adv. Mater. Res.*, **284–286**, 1477 (2011).
8. M. H. Kang, J. Song, H. Zhu, and S. Jiao, *Metall. Mater. Trans. B*, **46**, 162 (2015).
9. Y. Song, S. Jiao, L. Hu, and Z. Guo, *Metall. Mater. Trans. B*, **47**, 804 (2016).
10. S. Wang, C. Wan, X. Liu, and L. Li, *Metall. Mater. Trans. E*, **2**, 250 (2015).
11. S. Tokumoto, E. Tanaka, and K. Ogisu, *J. Met.*, **27**, 18 (1975) .
12. J. G. Gussone and J. M. Hausmann, *J. Appl. Electrochem.*, **41**, 657 (2011).
13. A. Kishimoto, Y. Yamada, K. Funatsu, and T. Uda, *Adv. Eng. Mater.*, **22**, 1900747 (2019).
14. K. Matiašovsky, Ž. Lubyovà, and V. Daněk, *Electrodepos. Surface Treat.*, **1**, 43 (1972).
15. J. De Lepinay, J. Bouteillon, S. Traore, D. Renaud, and M. J. Barbier, *J. Appl. Electrochem.*, **17**, 294 (1987).
16. A. Robin, J. De Lepinay, and M. J. Barbier, *J. Electroanal. Chem.*, **230**, 125 (1987).
17. A. Robin, *Mater. Lett.*, **34**, 196 (1998).
18. A. Robin and R. B. Ribeiro, *J. Appl. Electrochem.*, **30**, 239 (2000).
19. M. E. Sibert and M. A. Steinberg, *J. Electrochem. Soc.*, **102**, 641 (1955).
20. J. G. Wurm, L. Gravel, and R. J. A. Potvin, *J. Electrochem. Soc.*, **104**, 301 (1957).
21. D. Wei, T. Tada, and T. Oki, *ISIJ Int.*, **33**, 1016 (1993).
22. D. Wei, M. Okido, and T. Oki, *J. Appl. Electrochem.*, **24**, 923 (1994).
23. J. H. von Barner, P. Noye, A. Barhoun, and F. Lantelme, *J. Electrochem. Soc.*, **152**, C20 (2005).
24. V. V. Malyshev and D. B. Shakhnin, *Mater. Sci.*, **50**, 80 (2014).
25. Y. Norikawa, K. Yasuda, and T. Nohira, *Mater. Trans.*, **58**, 390 (2017).
26. Y. Norikawa, K. Yasuda, and T. Nohira, *Electrochemistry*, **86**, 99 (2018).
27. Y. Norikawa, K. Yasuda, and T. Nohira, *J. Electrochem. Soc.*, **166**, D755 (2019).
28. M. A. Steinberg, S. S. Carlton, M. E. Sibert, and E. Wainer, *J. Electrochem. Soc.*, **102**, 332 (1955).
29. F. Zhu, K. Qiu, and Z. Sun, *Electrochemistry*, **85**, 715 (2017).
30. N. Ene and S. Zuca, *J. Appl. Electrochem.*, **25**, 671 (1995).
31. J. Song, Q. Wang, X. Zhu, J. Hou, S. Jiao, and H. Zhu, *Mater. Trans.*, **55**, 1299 (2014).
32. G. Chen, M. Okido, and T. Oki, *Electrochim. Acta*, **32**, 1637 (1987).
33. G. J. Janz, M. R. Lorenz, and C. T. Brown, *J. Am. Chem. Soc.*, **80**, 4126 (1958).
34. K. Maeda, K. Yasuda, T. Nohira, R. Hagiwara, and T. Homma, *J. Electrochem. Soc.*, **162**, D444 (2015).
35. M. W. Chase (ed.), *NIST-JANAF Thermochemical Tables* (American Chemical Society, and the American Institute of Physics for the National Institute of Standards and Technology, New York) 4th ed. (1998).
36. M. S. Krause Jr and L. Ramaley, *Anal. Chem.*, **41**, 1365 (1969).
37. L. Ramaley and M. S. Krause Jr, *Anal. Chem.*, **41**, 1362 (1969).
38. J. J. O'Dea, J. Osteryoung, and R. A. Osteryoung, *Anal. Chem.*, **53**, 695 (1981).
39. K. Aoki, K. Tokuda, H. Matsuda, and J. Osteryoung, *J. Electroanal. Chem.*, **207**, 25 (1986).
40. J. R. Rumble Jr, *CRC Handbook of Chemistry and Physics* (CRC Press, Boca Raton, FL) 99th ed. (2018).
41. R. S. Nicholson and I. Shain, *Anal. Chem.*, **36**, 706 (1964).
42. G. J. Janz, *J. Phys. Chem. Ref. Data*, **17**, 136 (1988).
43. F. Lantelme, K. Kuroda, and A. Barhoun, *Electrochim. Acta*, **44**, 421 (1998).
44. J. Song, J. Xiao, and H. Zhu, *J. Electrochem. Soc.*, **164**, E321 (2017).
45. A. Girginov, T. Z. Tzvetkoff, and M. Bojinov, *J. Appl. Electrochem.*, **25**, 993 (1995).
46. K. Sakai and T. Nakamura, *Phys. Chem. Liq.*, **14**, 67 (1984).
47. R. D. Shannon, *Acta. Cryst.*, **A32**, 751 (1976).